



SYNTHESIS CONTROL AND CHARACTERIZATION OF HYDROXYAPATITE CERAMIC USING A SOLID STATE REACTION

Rungsarit Koonawoot¹, Cherdsak Saelee¹, Sakdiphon Thiansem², Sittiporn Punyanitya^{3,4*}

¹Department of Physic and Materials science, Faculty of Science, Chiang Mai University, Chiang Mai 50200, Thailand

²Department of Industrials Chemistry, Faculty of Science, Chiang Mai University, Chiang Mai 50200, Thailand

³Department of Surgery, Faculty of Medicine, Chiang Mai University, Chiang Mai 50200, Thailand

⁴Excellent center of Biomaterial and Medical Instrument, Research and Development of Science and Technology Institute, Chiang Mai University, Chiang Mai 50200, Thailand

*e-mail: punyanitya@hotmail.com

Abstract

In this study, hydroxyapatite (HA) powders were synthesized by a solid state reaction method. Calcium carbonate (CaCO_3) and ammonium dihydrogen phosphate ($\text{NH}_4\text{H}_2\text{PO}_4$) were used as the precursors. Powders were then uniaxially pressed and finally sintered at 1150°C, 1200°C, 1250°C and 1300°C for 2, 3 and 5 hours. The observed phases of the synthesised HA were dependent on the composition of calcium and phosphorus, temperature and soaking time. The powders samples were characterized by X-ray diffraction analysis (XRD), TG-DTA analysis, scanning electron microscopy (SEM) and infrared spectroscopy analysis (IR). A quantitative measurement from XRD showed that the main components of powder were HA phase and other phases were tricalcium phosphate and calcium oxide.

Keywords: hydroxyapatite, tricalcium phosphate, solid state reactions, X-ray diffraction analysis, IR spectroscopy

Introduction

Hydroxyapatite ($\text{Ca}_{10}(\text{PO}_4)_6(\text{OH})_2$, (HA)) is one of the most effective biocompatible materials and it is found to be the major component of bone. It is widely used in biological materials due to the apatite-like structure of enamel, dentin and bones, known as “hard tissue” (Rezwan et al. 2006). The chemical is pure HA crystals in the monoclinic space group $\text{P}2_1/\text{b}$ (Elliott et al. 1973). However, at temperatures above $\sim 250^\circ\text{C}$, there is a monoclinic to hexagonal phase transition in the HA (space group $\text{P}6_3/\text{m}$) (Elliott 1994). It is interpreted in terms of the aggregation of $\text{Ca}_9(\text{PO}_4)_6$ clusters, the so-called Posner’s clusters, that have been widely used since the publication of an article by Posner and Betts (Posner and Betts. 1975). The $\text{Ca}_9(\text{PO}_4)_6$ clusters appeared to be energetically favored in comparison to alternative candidates, including tricalcium phosphate ($\text{Ca}_3(\text{PO}_4)_2$), (TCP)) and $\text{Ca}_6(\text{PO}_4)_4$ clusters (Treboux et al. 2000). In hexagonal HA, the hydroxide ions are more disordered within each row when compared with the monoclinic form, pointing either upwards or downwards in the structure. This induces strains that are compensated by substitutions or ion vacancies. Some impurities, like partial substitution of hydroxides by fluoride or chloride, stabilize the hexagonal structure of HA at ambient temperatures. For this reason, hexagonal HA is seldom the stoichiometric phase, and it is very rare that single crystals of natural HA exhibit the hexagonal space group. A shell model was developed to study the lattice dynamics of HA, while a cluster growth model was created to illustrate its growth (Onuma and Ito 1998).

There are two sources of apatite mineral: the first one from biological and the second one from mineral deposits such as phosphate rock or phosphorite. A sedimentary rock is the essential mineral components which are carbonate fluoroapatite (McConnell 1973). HA can be prepared by several synthetic routes including solid state reactions (Yang and Wang 1998), chemical precipitation (Tadic et al. 2002), hydrothermal reactions (Jinawath et al. 2002), sol-gel methods (Chai et al. 1998) and mechanochemical methods (Nasari –Tabrizi and Fahami 2009) by using different calcium and phosphorus containing initial materials.

In the present study, HA ceramic was synthesized by solid state method with the following three aims: to form HA from mixing of CaCO_3 and $\text{NH}_4\text{H}_2\text{PO}_4$ by a solid state reaction, to study trends of HA phase formation, and to study the powder characteristics.

Methodology

The mixed powder was prepared by mixing the compositions of the calcium and phosphate at molar ratio 1.67. The synthesis process is based on two basic solid state reactions of CaCO_3 (analytical grade, Ajax, Netherland) with $\text{NH}_4\text{H}_2\text{PO}_4$ (analytical grade, Merck, Germany).

An appropriate composition of mixture as mixed by high a speed grinder in a dry state for 45 minutes. The experimental conditions for all samples are presented in Table 1. A mixture of composites was pressed uniaxially into pellets 2 mm thick and 15 mm in diameter under typical stresses of 3 MPa in a stainless steel die. The die walls were lubricated using a liquid solution of 5 wt% stearic acid in ethanol. The green pellets were sintered at temperatures of 1150°C, 1200°C, 1250°C and 1300°C for 2, 3 and 5 hours in a Eurotherm furnace 3504. The samples were characterized using scanning electron microscopy (SEM-JEOL JEM-2010), X-ray diffraction (XRD-Bruker Advance 8D), Fourier transform infrared spectroscopy (FTIR-Thermo Nicolet).

Table 1 Sample identifications and experimental conditions

Sample	H1	H2	H3	H4	H5	H6	H7	H8	H9	H10	H11	H12
Temperature (°C)	1150	1150	1150	1200	1200	1200	1250	1250	1250	1300	1300	1300
Soaking time (hours)	2	3	5	2	3	5	2	3	5	2	3	5

Results

Powder analysis.

The X-ray diffraction pattern of CaCO_3 precursor before mixing was the form of the mineral calcite. No other phases were found that compared with the diffraction pattern of JCPDS card No. 085-1108 of calcite (Figure 1) (Board and Love 1979). The size of particles and specific surface areas of reaction material is shown in Table 2. (Malvern Particle Size Analyzer, Mastersizer S, Ver. 2.19).

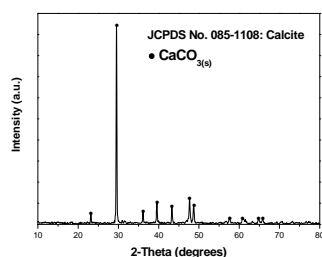


Figure 1 XRD pattern of CaCO_3

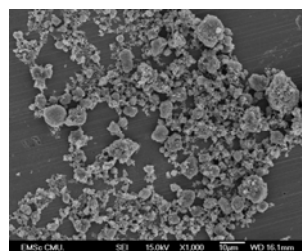


Figure 2 SEM micrograph of mixture powder

Table 2 Distributions of mixture powders before and after grinding

Starting powders	D (v,0.5) (μm)	D (v,0.9) (μm)	D (4,3) (μm)	Specific S.A. (m^2/g)
Before grinding				
$\text{CaCO}_3(\text{s})$	13.32 ± 0.08	43.35 ± 0.18	18.29 ± 0.08	1.1373 ± 0.003
$\text{NH}_4\text{H}_2\text{PO}_4(\text{s})$	14.43 ± 0.09	78.98 ± 8.20	22.91 ± 0.09	0.5761 ± 0.004
After 45 mins grinding				
Mixture of $\text{CaCO}_3(\text{s})$ and $\text{NH}_4\text{H}_2\text{PO}_4(\text{s})$	5.32 ± 0.03	29.45 ± 0.13	11.04 ± 0.06	3.7228 ± 0.01

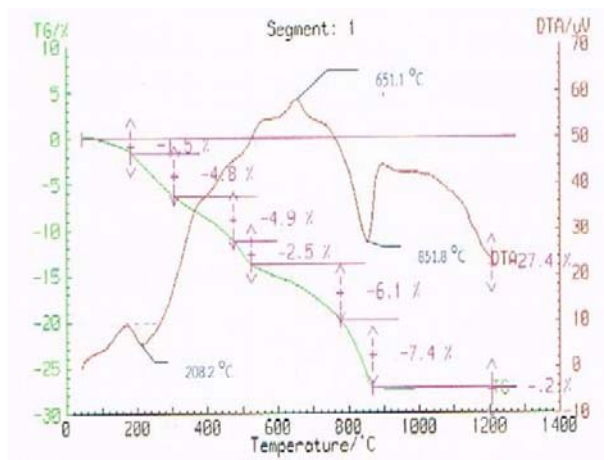
Note: D (v,0.5) is the diameter where 50% of the distribution is above and 50% is below. D(v,0.9) is 90% of the volume distribution is below this value. D[4,3] is the equivalent volume mean diameter. Specific S.A (m^2 per gram) of the test particles (Dodge 1984).

This result showed that volume mean diameter of the tested particles of 11.04 ± 0.06 can be prepared through mixture powder by a solid state reaction. The specific surface areas of powder had increased as $3.7228 \pm 0.01 \text{ m}^2/\text{g}$. After 45 minutes grounding the mixture powders occur agglomerates of particles that shown by SEM image in Figure 2.

Thermal analysis.

Table 3 The detail of DTA and TG data

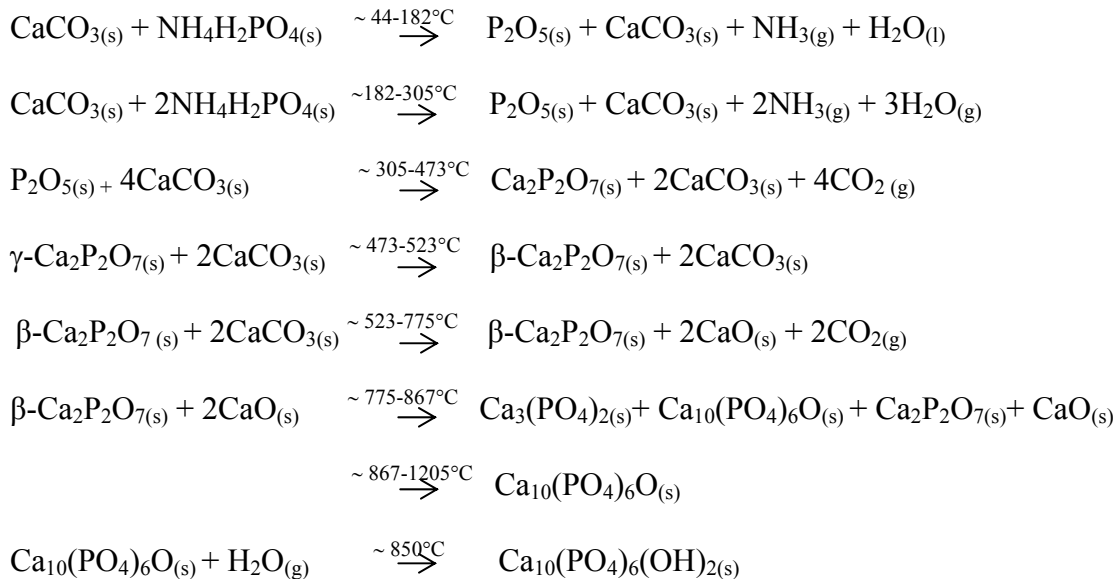
DTA	
Type of reaction	Temperature ($^{\circ}\text{C}$)
Endothermic	208.2
Endothermic	851.8
Exothermic	651.1
TG	
Temperature range of weight loss ($^{\circ}\text{C}$)	Weight loss (%)
43.5-182.2	1.5
182.2-305.5	4.8
305.5-473.2	4.9
473.2-523.4	2.5
523.4-775.5	6.1
775.5-867.7	7.4
867.7-1205.4	0.2
Total weight loss	27.4

**Figure 3** DTA/TG analyses curves of formation of mixture powder

Thermal analysis is important to know materials reactivity under specific temperature. The TG curve can be divided into seven weight loss steps in Table 3. The thermogram of mixed powder showed continuously endothermic and exothermic evolution and three distinct thermal events during the reaction of CaCO_3 and $\text{NH}_4\text{H}_2\text{PO}_4$, mixed in a composition of precursors to form HA in Figure 3.

The solid state reaction between CaCO_3 and $\text{NH}_4\text{H}_2\text{PO}_4$ mixed in a Ca/P molar ratio 1.67 to form HA main phase and secondary phase as TCP and CaO. The first endothermic peak over

182.2 to 305.5°C is due to the ammonia and water loss, in weight loss ~ 4.8 wt%. The second exothermic event took place temperature range 523.4 to 775.5°C that shown in the DTA curve of Figure 3, due to the reaction of P₂O₅ and CaCO₃ to form the intermediary compound Ca₂P₂O₇, by the elimination of the CO₂ in weight loss ~ 6.1 wt.%. The third endothermic peak over 775.5 to 867.7°C is due to starts decompose of the carbonate transform to CaO and CO₂ gas released in weight loss ~ 7.4 wt%. The process continues during until at 851.8°C exist the decomposed of the carbonate and weight loss 7.4 wt%. The total observed weight loss is 27.4 wt% upon heating to 1200°C. The endothermal peak during heating and the exothermal peak during cooling correspond to loss of water from pure HA and absorption of moisture by oxyapatite. The detailed solid state reaction sequence between the starting powders upon heating can be concluded as follows (Yang and Wang 1998):



XRD analysis

Effect of sintering temperature and soaking time on phase formation of sintered samples.

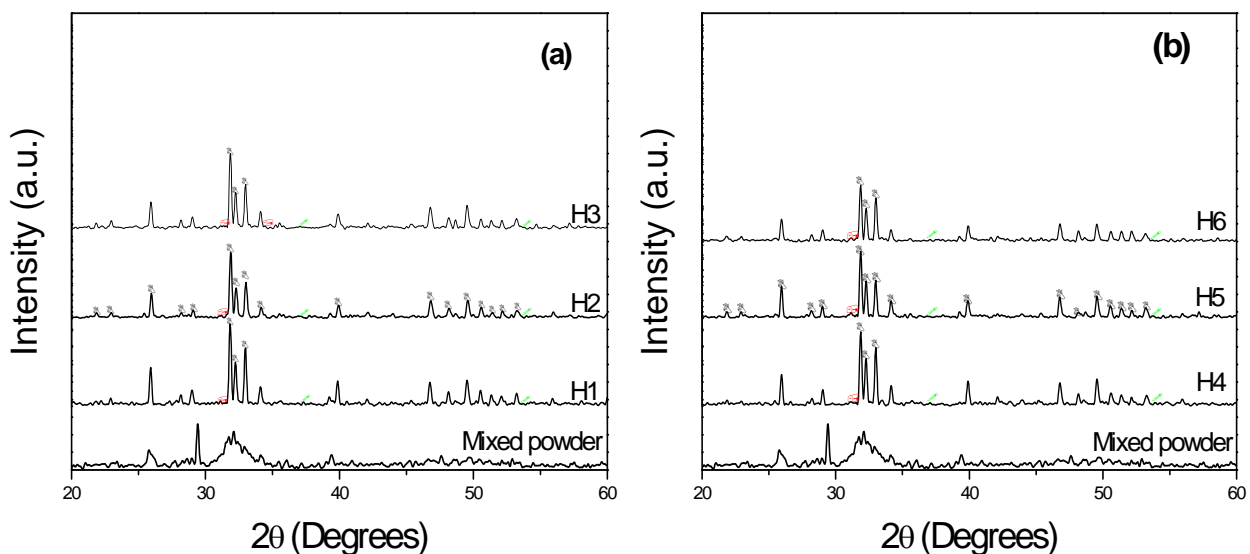


Figure 4 XRD patterns of the sintered samples at (a) 1150°C and (b) 1200°C for 2, 3 and 5 hours, B: HA, :, !: CaO

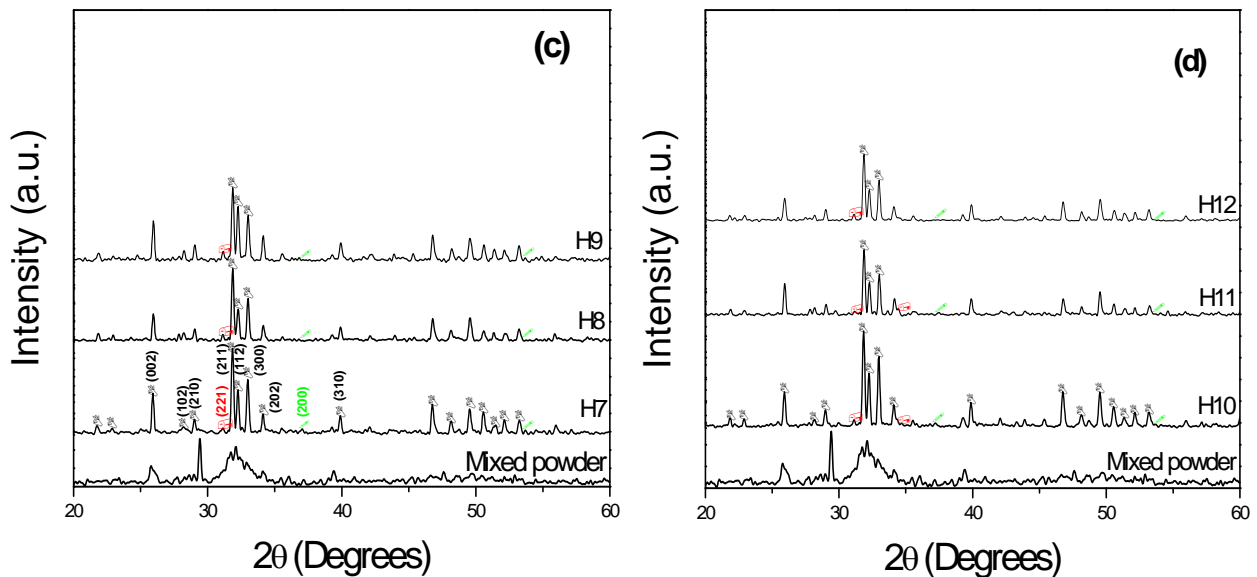


Figure 5 XRD patterns of the sintered samples at (c) 1250°C and (d) 1300°C for 2, 3 and 5 hours, B: HA, \circ : TCP, \triangle : CaO

XRD results of samples of synthesized HA powder before thermal treatment as mixed powder. The broadening peak of the crystalline cannot be identified to HA, JCPDS no. 09-0432 (Markovic et al. 2004). The results show that a mixed powder presence of the poorly crystalline HA phases (Mavropoulos et al. 2003; Porter et al. 2003). The low crystallinity characteristic can be reduced by thermal treatment and soaking time to form a solid entity (Liou et al. 2003). Figure 4(a) and (b) show the XRD patterns of the sintered samples at 1150°C and 1200°C for 2, 3 and 5 hours. Figure 5(c) and (d) show the XRD patterns of the sintered samples at 1250°C and 1300°C for 2, 3 and 5 hours. Results of the study contained phase HA, TCP (JCPDS no. 09-169) and CaO (JCPDS no. 37-1497) (Ermiş and Peters 2006). The peaks of HA, TCP and CaO are indexed according to standard patterns the XRD patterns. The intensity of HA peaks was noticeably increased when the appropriate sintering schedule. However, for all condition of samples showed an intensity of HA crystal peaks was not significantly increased by increasing sintering time. It seems that the sintering time showed a less pronounced effect on the crystallinity of the HA sample. Simultaneously, the sintering temperature played a considerable role in the phase formation of HA (Monmaturapoj and Yatongchai 2010). The intensity of (002), (102), (210), (211), (112), (300), (202) and (310) lattice plane of HA, (221) lattice plane of TCP and (200) lattice plane of CaO on the XRD patterns of solid-state reaction method. This method was used as a direct indicator of its purity (Afshar et al. 2003).

The percentages of volume fraction of HA, TCP and CaO present in all the samples were calculated using the relative intensity ratio (RIR) of the main diffraction peaks of HA ($2\theta = 31.8$), TCP ($2\theta = 31.0$) and CaO ($2\theta = 37.4$) (Raynaud et al. 2001). The relative intensity ratios corresponding to the major phases observed in the XRD patterns of powders sintered at different were computed using the association given in equation 1.

$$\text{RIR} = \frac{I_{\beta\text{-TCP}}}{I_{\beta\text{-TCP}} + I_{\text{HA}}} \quad (1)$$

The percentage of each phase present was calculated by using Equation 1. Table 4 shows the result of phase composition.

Table 4 Phase composition for sintered samples

Sample	Composition (%)		
	HA	TCP	CaO
H1	89.10	5.49	5.40
H2	90.57	5.47	3.97
H3	89.98	4.01	6.00
H4	89.86	4.24	5.90
H5	90.27	5.67	4.06
H6	89.02	6.61	4.37
H7	91.23	5.27	3.51
H8	87.26	7.67	5.07
H9	88.61	7.14	4.25
H10	89.97	5.67	4.36
H11	89.67	7.11	3.22
H12	87.20	8.62	4.18

Sample H7 is showed the optimum of percentage of HA phase have the highest with 91.23%. Besides that, it is also contained 5.27% of TCP and 3.51% of CaO.

SEM analysis.

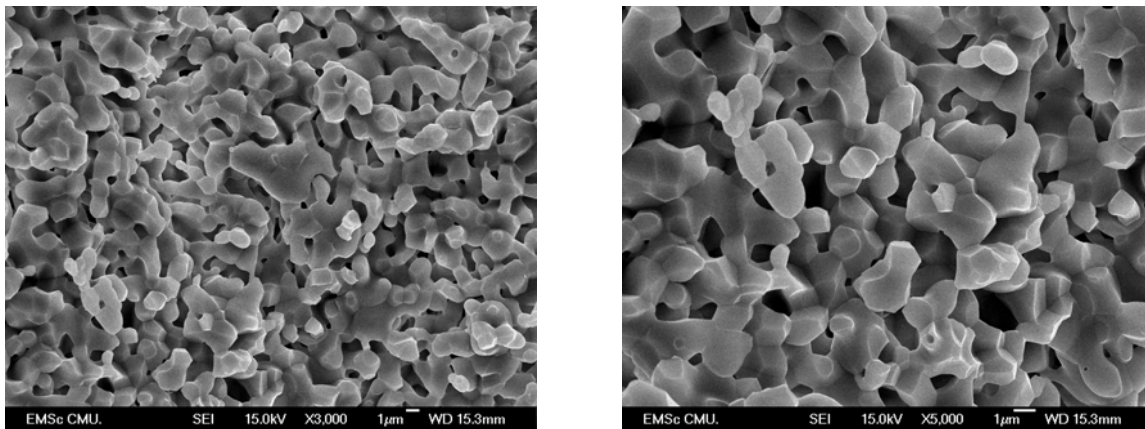


Figure 6 SEM images of sintered samples at 1250°C for 2 hr. at $\times 3,000$ (left) and $\times 5,000$ (right)

The microstructure was accompanied by the small pores which always exist on grain boundaries and enclosed by several grains in the proximity as present in this Figure 6. In densification process, therefore, sintering temperature has a more crucial effect than sintering time on synthesis HA ceramic of samples. The microstructural observations of sintered materials showed the homogeneous with an average grain size of about 1 μm and the material containing TCP and CaO was similar.

FTIR analysis.

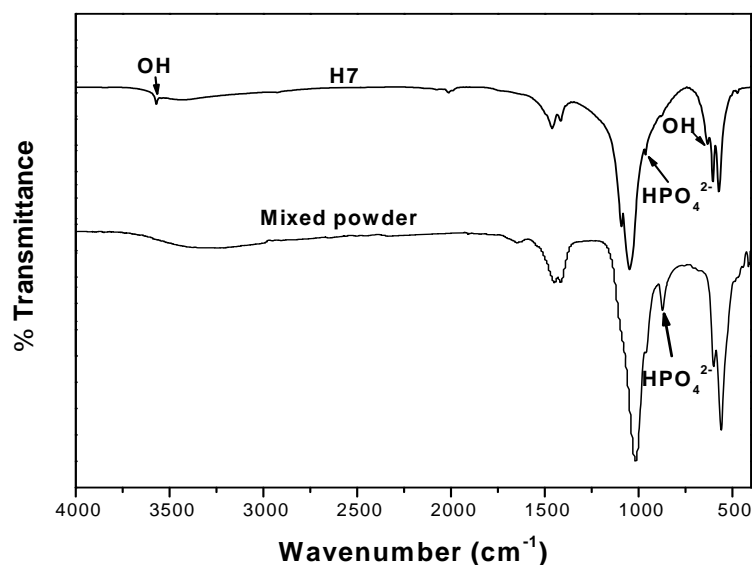


Figure 7 FTIR spectra of mixed powder and sample H7

The FTIR spectra of mixture powder before thermal treatment is shown the weak absorption peak at 873 cm^{-1} was assigned to the P-O-H vibration in the HPO_4^{2-} group (Yubao et al. 1994), which exists in nonstoichiometric HA. Sample H7 was showed to spectra illustrate the hydroxyl bond stretch at 3570 cm^{-1} and HPO_4^{2-} at 963 cm^{-1} corresponding to HA and TCP structure respectively. IR absorption spectra of the sample H7 sintered at different temperatures for 2 hours are shown characteristic absorption band of OH^- at 636 cm^{-1} increased with increasing sintering temperature in figure 7, while the absorption peaks of PO_4^{3-} at 602 cm^{-1} and 570 cm^{-1} . According, the optimum heat treatment conditions for preparing pure HA are sintering at 1250°C for 2 hr.

Discussion and Conclusion

In the above studies, HA ceramic was synthesized by solid-state reaction methods with different temperatures. Secondary phases were occurred TCP and CaO all samples. The purity of the synthesized HA powders are from 87.20% to 91.23% according to the composition of calcium with phosphorus, temperature and time. The optimum heat treatment conditions are sintering for 2 hr. at 1250°C for HA. The crystallinity of the material was largely increased by thermal treatment and directly influenced the appearing of TCP and CaO secondary phases. The amorphous phase remained in lower amount after thermal treatment. The control of the stoichiometry of compounds obtained from HA powder synthesis often has been difficult. HA powder synthesis usually gives with relative ease compounds that are slightly nonstoichiometric (Young and Holcomb 1982). This studied interested in reaction sintering mainly to systems in which the products are solids at the appropriate sintering temperature and time. The energy changes for chemical reaction are much larger than those for surface area changes and it would be very desirable if the free energy of the reaction could be used to drive the densification process. Nonetheless, there is no evidence that the energy of the reaction can act directly as a driving force for densification. Reaction sintering has the benefit of eliminating the pre-reaction (or calcination) step in the formation of solids with complex composition (Sacks et al. 1991).

A step forward is to study the strength and porosity of sample for study relation of suitable sintering schedule which effect to biomaterials applications.




Acknowledgements

This work was supported by The Faculty of Science and Graduate School Chiang Mai University, the Commission on Higher Education (CHE) and the Excellent Center of Biomaterial and Medical Instrument, Research and Development of Science and Technology Institute, Chiang Mai University, Department of Physics and Materials sciences, Faculty of Science, Chiang Mai University, Chiang Mai University are acknowledged for their support.

References

1. Rezwan K, Chen QZ, Blaker JJ, Boccaccini AR (2006) Biodegradable and bioactive porous polymer/inorganic composite scaffolds for bone tissue engineering. *Biomaterials* 27:3413–3431.
2. Elliott JC (1994) Structure and chemistry of the apatites and other calcium orthophosphates. *Studies in inorganic chemistry Elsevier: Amsterdam, Netherlands* 18:389.
3. Treboux G, Layrolle P, Kanzaki K, Onuma K, Ito A (2000) Existence of Posner's cluster in vacuum. *Journal of Physical Chemistry A* 104: 5111-5114.
4. Onuma K, Ito A (1998) Cluster growth model for hydroxyapatite. *Chemistry of Materials* 10: 3346-3351.
5. McConell D (1973) Apatite: its crystal chemistry, mineralogy, utilization, and biologic occurrence. Berlin, Springer-Verlag.
6. Yang X, Wang Z (1998) *Journal of Material Chemistry* 8:2233.
7. Tadic D, Peters F, Epple M (2002) *Biomaterials* 23:2555.
8. Jinawath S, Polchai D, Yoshimura M (2002) *Material Science and Engineering C* 22:35.
9. Chai CS, Gross KA, Nissan BB (1998) *Biomaterials* 19:2291.
10. Nasari –Tabrizi B, Fahami A (2009) *Material Letter* 63:543.
11. Board RG, Love G (1979) *Comparative Biochemistry and Physiology* 66:667-672.
12. Dodge LG (1984) Calibration of the Malvern particle sizer. *Applied optics* 23:2415-2419.
13. Yang X, Wang Z (1998) Synthesis of biphasic ceramics of hydroxyapatite and β -tricalcium phosphate with controlled phase content and porosity. *Journal of Material Chemistry* 8:2233-2237.
14. Markovic M, Fowler BO, Tung MS (2004) *Journal of Research of the National Institute of Standards and Technology* 11:533.
15. Mavropoulos E, Rossi AM, Rocha NCC, Soares GA, Moreira JC, Moure GT (2003) *Materials Characterization* 5578.
16. Ermrich M, Peters F (2006) *Z Kristallogr Supplement* 23:523.
17. Monmaturapoj N, Yatongchai (2010) Effect of sintering on Microstructure and Properties of Hydroxyapatite Produced by Different Synthesizing Methods. *Journal of Metals, Materials and Minerals* 20:53-61.
18. Afshar A, Ghorbani m, Ehsani N, Saeri MR, Sorrell CC (2003) *Materials and Design* 24:197-202.
19. Raynaud S, Champion E, Bernache-Assollant D, Laval JP (2001) Determination of Calcium/Phosphorus Atomic Ratio of Calcium Phosphate Apatites Using X-ray Diffractometry. *Journal of American ceramic society* 84: 359-366.
20. Yubao L, Klein CPAT, Xingdong Z, De Groot K (1994) Formation of a bone apatite-like layer on the surface of porous hydroxyapatite ceramics. *Biomaterials* 15:835-841.

- 
21. Young RA, Holcomb DW (1982) Variability of Hydroxyapatite Preparations. *Calcified Tissue International* 34:17-32.
 22. Sack MD, Bozkurt N, Scheiffele GW (1991) *Journal of American ceramic society* 74:2428.